arXiv:1512.04444v1 [physics.comp-ph] 14 Dec 2015

Variational Time Integration Approach for Smoothed Particle Hydrodynamics Simulation of Fluids

Leandro Tavares da Silva*[1,2] and Gilson Antonio Giraldi†[1]

[1]National Laboratory for Scientific Computing, Petrópolis 25651-075, Brazil.
[2]Federal Center of Technology Education Celso Suckow da Fonseca, Petrópolis 25620-003, Brazil.

December 15, 2015

Abstract

Variational time integrators are derived in the context of discrete mechanical systems. In this area, the governing equations for the motion of the mechanical system are built following two steps: (a) Postulating a discrete action; (b) Computing the stationary value for the discrete action. The former is formulated by considering Lagrangian (or Hamiltonian) systems with the discrete action being constructed through numerical approximations of the action integral. The latter derives the discrete Euler-Lagrange equations whose solutions give the variational time integrator. In this paper, we build variational time integrators in the context of smoothed particle hydrodynamics (SPH). So, we start with a variational formulation of SPH for fluids. Then, we apply the generalized midpoint rule, which depends on a parameter α, in order to generate the discrete action. Then, the step (b) yields a variational time integration scheme that reduces to a known explicit one if $\alpha \in \{0, 1\}$ but it is implicit otherwise. Hence, we design a fixed point iterative method to approximate the solution and prove its convergence condition. Besides, we show that the obtained discrete Euler-Lagrange equations preserve linear momentum. In the experimental results, we consider artificial viscous as well as boundary interaction effects and simulate a dam breaking set up. We compare the explicit and implicit SPH solutions and analyze momentum conservation of the dam breaking simulations.

1 Introduction

Fluid simulation involves numerous works that can be coarsely classified in PDEs and lattice based techniques. PDEs methods derive computational models based on continuous fluid equation, like the Navier-Stokes ones, and numerical techniques formulated through discretization approaches that can be Lagrangian (Smoothed Particle Hydrodynamics (SPH) [20], Moving Particle [14], Moving-Particle Semi-Implicit [2]), Eulerian (Finite Element, Finite Difference and Finite Volume) [1]. Lattice based approaches are built using cellular automata and lattice Boltzmann methods [5].

*leandros@lncc.br
†gilson@lncc.br

In this paper we focus on the SPH technique, that was originally invented to solve astrophysical problems in three dimensional open space [9, 25]. It is a meshfree, Lagrangian approach based on particle systems and interpolation theory. Kinematic and dynamic variables, such as velocity, density, deformation gradient and stresses are obtained from the fluid flow at the particle positions using interpolation functions known as kernels. Since its invention , SPH has been extensively studied and extended to address scientific and engineering problems in material science, free surface flows, explosion phenomena, heat transfer, mass flow, among many other applications (see [24] and references therein).

The dynamic model behind SPH is based on classical mechanics which is concerned with physical laws to describe the behavior of a macroscopic system under the action of forces [10]. For instance, when considering a particle system in the $3D$ space under the action of gravity, we can take the position vector of each particle along the time t, which in cartesian coordinates is given by $(x^{i1}, x^{i2}, x^{i3}) \in \mathbb{R}^3$, $i = 1, 2, \ldots, M$, and use the Newton's laws to get the governing equations written in terms of the cartesian coordinates and the time t. In a more general situation, the instantaneous configuration of each particle may be described by the values of n *generalized* coordinates $(q^{i1}, q^{i2}, \cdots, q^{in})$. So, we need a methodology to write the evolution equations of the system in terms of coordinates other than the cartesian ones.

The Lagrangian formulation of mechanics is a framework to address this issue. It is a variational approach based on the integral Hamilton's principle which states that the correct path of the motion of a system is a stationary value for the action integral [10]. The corresponding Lagrange's equations allow to write the evolution of the system, the SPH fluid particles in our case, in term of the generalized coordinates. Then, we update the velocities and positions of the particles by using a suitable time integrator. This methodology is followed by the variational approaches for SPH simulation of fluids found in the literature [4, 3].

In this paper we follow a different variational formulation, based on discrete mechanics concepts. The fundamental point of the theory of discrete mechanics consists of discretizing Hamilton's principle of Lagrangian mechanics [11]. Consequently, in discrete mechanics, the time evolution of the mechanical system is obtained following two steps: (a) Computing a discrete action; (b) Postulating that the corresponding path is a stationary value for the discrete action. The former is implemented by considering Lagrangian (or Hamiltonian) systems with the discrete action being constructed through numerical approximations of the action integral. The latter derives the discrete Euler-Lagrange equations whose solutions give the variational time integration technique [22].

In this paper, we derive variational time integrators in the context of SPH. Up to the best of our knowledge, such approach has not been used by the SPH community before. So, we start with the continuum variational formulation of SPH for fluids described in [3]. Then, we apply the generalized midpoint rule in order to build the discrete action [18]. This numerical integration rule depends on a parameter α which is further explored in the text. So, we show that the discrete Euler-Lagrange equations reduces to the known Verlet technique if $\alpha \in \{0, 1\}$. For $0 < \alpha < 1$ we obtain an implicit integration scheme. We demonstrate the sufficient condition to apply the contraction mapping principle and, consequently, to cast the implicit scheme as a method of successive approximations to get the solution. Momentum conservation is also demonstrated for the discrete Euler-Lagrange equations. In the implementation details, numerical aspects and boundary interaction effects are added to the discrete Euler-Lagrange equations. In the experimental results, we simulate a $2D$ dam breaking set up. We compare the explicit ($\alpha \in \{0, 1\}$) and the implicit SPH solution obtained by $\alpha = 0.5$, and analyze momentum conservation of the time integrators.

The remainder of this paper is organized as follows. Section 2 describes related works. The discrete Lagrangian mechanics is presented on section 3. Next, in section 4, we describe the Lagrangian formulation of SPH. The derivation of the variational time integrator for SPH is pre-

sented on section 5. This section also demonstrates the momentum conservation of the obtained discrete Euler-Lagrange equations (section 5.1) as well as the application of contraction mapping principle and implementation details (sections 5.2 and 5.3). The computational results and conclusions/future works are presented on sections 6 and 7, respectively.

2 Related Works

Variational integrators in mechanical systems start by considering mechanics from a variational point of view, following remarkable works of Lagrange and Hamilton [10]. The Hamilton's principle or the least action principle allows to cast the Newton's framework into a geometric viewpoint in which the path followed by the physical system in the configuration space has optimal geometric properties analogously to the notion of geodesics on curved surfaces [8]. Therefore, we can design numerical integrators that exploit the geometric structure behind mechanical systems, which are named geometric integrators [11, 8]. A special class of geometric integrators, called variational integrators, discretized the variational formulation of mechanics generating iterative schemes to compute an approximation for the path of the physical system with any order of accuracy. Besides, this discrete geometric framework can handle constraints, external and dissipative forces making variational integrators both versatile and powerful [12, 18, 17].

In the Lagrangian point of view, given a mechanical system with configuration space (manifold) Q, the Lagrangian itself is a real map defined in the velocity phase space. The first step to represent the system in discrete variational mechanics frameworks is to replace the velocity phase space by $Q \times Q$ through some integration rule in order to convert the continuous action in a discrete one. However, the Noether's theorem allows to characterize the essence of a mechanical system through its symmetries and invariants. Thus preserving these symmetries and invariants into the discrete computational approaches is fundamental to properly capture the correct continuous motion. In fact, it can be shown that invariants can be preserved by variational time integrators due to the fact that they respect variational nature of dynamics [17]. This property, together with the fact that variational approaches gives an unified view on both discrete mechanics and integration methods for mechanical systems motivate the application of these frameworks for computational models in solids [18, 23], optimal control [6], n-body problems [16], computer animation [13, 26] and celestial mechanics [15].

The key elements in variational time integrators are the discrete action sum, the discrete Euler-Lagrange equations and the discrete Noether's theorem that were clearly understood due to early works (see [22] and references therein). Numerical aspects and convergence properties were specifically considered in [12, 27].

On the other hand, traditional SPH formulations for fluids rely on standard conservation equations and a particle framework to discretize the corresponding Navier-Stokes equations, generating models that treat the continuum fluid as a system of particles and recover continuous fields by using interpolation kernels [28]. Variational formulations of SPH for fluid applications have been proposed, where the constitutive equation of the fluid is given by an internal energy term which is a function of the density [4, 3]. These formulations provide a basis to discuss momentum preserving properties of SPH approaches. In this paper, they are used to derive variational time integrators for SPH by computing the discrete action and its stationary point, as we shall see in the next sections.

3 Discrete Lagrangian Mechanics

Let us consider a physical system whose instantaneous configuration may be described by the values of n generalized coordinates $\mathbf{q} = (q^1, q^2, \cdots, q^n)$ which is a point in a $n - dimensional$

Cartesian hyperspace known as *configuration space*. As time goes on from a time t_1 to a time t_2, the system changes its configuration due to internal and external forces. Therefore, the evolution of the system can be seem as a continuous path $\mathbf{q}(t)$, in the configuration space, parameterized through the time t.

The Hamilton's principle gives a methodology to write the evolution equation of the system in terms of the generalized coordinates and time t. So, given the kinetic energy $K = K(\dot{\mathbf{q}})$, where $\dot{\mathbf{q}} = d\mathbf{q}/dt$, and a scalar potential $P(\mathbf{q}, \dot{\mathbf{q}}, t) = U(\mathbf{q}) + V(\mathbf{q}, \dot{\mathbf{q}}, t)$, where U and V accounts for conservative and non-conservative velocity-dependent forces, the Hamilton's principle states that the motion of the system from time t_1 to time t_2 is such that the line integral:

$$S(\mathbf{q}) = \int_{t_1}^{t_2} L(\mathbf{q}, \dot{\mathbf{q}}, t)\, dt, \tag{1}$$

where $L(\mathbf{q}, \dot{\mathbf{q}}, t) = T(\dot{\mathbf{q}}) - U(\mathbf{q}) - V(\mathbf{q}, \dot{\mathbf{q}}, t)$, named the Lagrangian of the system, has a stationary value for the correct path of the motion [10].

In discrete mechanics, we derive the governing equations of a physical system by firstly considering a time sequence $t_0, t_1, \ldots, t_N$ to write: $\mathbf{q}(t_0) \equiv \mathbf{q}_0$, $\mathbf{q}(t_1) \equiv \mathbf{q}_1, \cdots, \mathbf{q}(t_N) \equiv \mathbf{q}_N$.

In this way, the system evolution is represented by a discrete trajectory $(\mathbf{q}_k, t_k)$, $k = 0, 1, \ldots, N$, and the action in equation (1) becomes the *discrete action*, given by:

$$S_d(\mathbf{q}_0, \mathbf{q}_1, \ldots, \mathbf{q}_N) = \sum_{k=0}^{N-1} L_d(\mathbf{q}_k, \mathbf{q}_{k+1}), \tag{2}$$

where:

$$L_d(\mathbf{q}_k, \mathbf{q}_{k+1}) \approx \int_{t_k}^{t_{k+1}} L(\mathbf{q}, \dot{\mathbf{q}}, t)\, dt. \tag{3}$$

is called the *discrete Lagrangian*.

So, we can get a discrete version of the Hamilton's principle by considering a family $\mathbf{q}_k(\varepsilon)$, $k = 0, 1, 2, \ldots N$ such that $\mathbf{q}_0(\varepsilon) = \mathbf{q}_0$ and $\mathbf{q}_N(\varepsilon) = \mathbf{q}_N$, for all ε (end points fixed). So, in this case:

$$S_d(\mathbf{q}_0(\varepsilon), \mathbf{q}_1(\varepsilon), \ldots, \mathbf{q}_N(\varepsilon)) = S_d(\varepsilon),$$

and:

$$\delta S_d \equiv \left(\frac{dS_d(\varepsilon)}{d\varepsilon}\right)_{\varepsilon=0} = \sum_{i=0}^{N} \frac{\partial S_d}{\partial \mathbf{q_i}} \delta \mathbf{q}_i, \tag{4}$$

where:

$$\delta \mathbf{q}_i = \left(\frac{d\mathbf{q_i}}{d\varepsilon}\right)_{\varepsilon=0},$$

Finally, analogously to the continuous case, we postulate that the desired (discrete) path must satisfies $\delta S_d(\mathbf{q}) = 0$, which renders:

$$\frac{\partial}{\partial \mathbf{q}_k} L_d(\mathbf{q}_{k-1}, \mathbf{q}_k) + \frac{\partial}{\partial \mathbf{q}_k} L_d(\mathbf{q}_k, \mathbf{q}_{k+1}) = 0, \tag{5}$$

for $k = 1, 2, \ldots, N-1$, which are the discrete Euler-Lagrange equations [22].

4 Lagrangian Formulation for SPH

The two fundamental elements in the SPH method are an interpolation kernel $W : \mathbb{R}^3 \to \mathbb{R}^+$, which is a symmetric function respect to the origin $(0, 0, 0)$, limited, with compact support, and a particle system $\mathbf{q}^i = (x^{i1}, x^{i2}, x^{i3}) \in \mathbb{R}^3$, $i = 1, 2, \ldots, M$, that represents a discrete version (sample) of the fluid. The kernel estimate of a scalar quantity A and its gradient in a point $\mathbf{q}^i \in \mathbb{R}^3$ are given by [20]:

$$\left\langle A(\mathbf{q}^i)\right\rangle = \sum_{j=1}^{M} \frac{m_j}{\rho(\mathbf{q}^j)} A(\mathbf{q}^j) W(\mathbf{q}^i - \mathbf{q}^j, h), \tag{6}$$

$$\left\langle \nabla A(\mathbf{q}^i)\right\rangle = \sum_{j=1}^{M} \frac{m_j}{\rho(\mathbf{q}^j)} A(\mathbf{q}^j) \nabla_i W(\mathbf{q}^i - \mathbf{q}^j, h), \tag{7}$$

where $\nabla_i W(\mathbf{q}^i - \mathbf{q}^j, h)$ means $\nabla_{\mathbf{r}} W(\mathbf{r} - \mathbf{q}^j, h)$ evaluated at $\mathbf{r} = \mathbf{q}^i$, h is the smoothing length which determines the support of the kernel and $\rho(\mathbf{q}^j)$ is the density at the particle position $\mathbf{q}^j$ [20]. Therefore, the kernel estimate of the density at the position $\mathbf{q}^i$ is:

$$\left\langle \rho\left(\mathbf{q}^i\right)\right\rangle = \sum_{j=1}^{M} m_j W(\mathbf{q}^i - \mathbf{q}^j, h), \tag{8}$$

Besides, we can show that the divergent for a vector field $\mathbf{v}$ can be computed as [20]:

$$\left\langle \nabla\cdot\mathbf{v}(\mathbf{q}^i)\right\rangle = \sum_{j=1}^{M} \frac{m_j}{\rho(\mathbf{q}^j)} \left(\mathbf{v}\left(\mathbf{q}^j\right) - \mathbf{v}\left(\mathbf{q}^i\right)\right) \nabla_i W(\mathbf{q}^i - \mathbf{q}^j, h), \tag{9}$$

For simplicity, in what follows, we take off the brackets in the left hand side of expressions (6)-(8). In this work, the kernel function adopted is the Gaussian one:

$$W(R) = \ell e^{-R^2}, \tag{10}$$

where ℓ is a constant. Also, in the SPH framework it is usually postulated a state equation that correlates density and pressure, which in this work is given by:

$$p(\mathbf{q}^i) = B\left[\left(\frac{\rho(\mathbf{q}^i)}{\rho_0}\right)^7 - 1\right], \tag{11}$$

where ρ_0 is the rest density and B is a constant, such that $B = c^2\rho_0/7$, where is the speed sound in fluid.

The SPH model for a fluid can be seen as a system composed by particles $\mathbf{q}^i = (x^{i1}, x^{i2}, x^{i3})$ subject to forces derived from internal and external potentials that are functions of fluid fields like density ρ, pressure p, and velocity $\mathbf{v}$. Moreover, the configuration of the SPH system along the time is described by a continuous path in the configuration space:

$$\mathbf{q}(t) = \left(\left\{\mathbf{q}^1(t)\right\}^T, \left\{\mathbf{q}^2(t)\right\}^T, \cdots, \left\{\mathbf{q}^M(t)\right\}^T\right)^T \in \mathbb{R}^{3M}. \tag{12}$$

Such viewpoint is behind the (continuum) variational formulation of SPH presented in [4, 3]. The total kinetic energy of the system can be simply computed as the sum of the kinetic energy of the particle:

$$K(\mathbf{q}) = \frac{1}{2}\sum_{i=1}^{M} m_i(\dot{\mathbf{q}}^i \cdot \dot{\mathbf{q}}^i) \tag{13}$$

The potential energy is the sum of total external energy and the total internal energy:

$$P(\mathbf{q}) = \Pi_{\text{ext}} + \Pi_{\text{int}} \tag{14}$$

Thus, for the case where the external forces results form a gravitational field $\mathbf{g}$, the total external energy is

$$\Pi_{\text{ext}} = -\sum_{i=1}^{M} m_i(\mathbf{q}^i \cdot \mathbf{g}), \tag{15}$$

On the other hand, the internal energy will incorporate the constitutive characteristics of the continuum; the fluid in this case. In general, it is possible to express the total internal energy as the sum:

$$\Pi_{\text{int}} = \sum_{i=1}^{M} \pi(\rho\left(\mathbf{q}^i\right), \cdots) \tag{16}$$

where π will depend on the deformation, density or other constitutive parameters. In [3] the constitutive equations for a nearly incompressible flow without dissipative effects is:

$$\frac{d\pi}{d\rho} = \frac{p}{\rho^2}, \tag{17}$$

where p is the fluid pressure. In [4, 3] expressions (13)-(17) are used to compute the (continuous) Lagrangian:

$$L = K - \Pi_{\text{int}} - \Pi_{\text{ext}}, \tag{18}$$

and the governing equations of the SPH system of particles can be yielded through the (continuous) Euler-Lagrange equations. Instead, in this work we follow a discrete approach described next.

5 SPH Variational Time Integrator

To derive the discrete variational formulation for SPH systems we need to build a discrete Lagrangian through expression (3) and then insert the result in the discrete Euler-Lagrange equations (5). Following section 3, we consider a time sequence $t_0, t_1, \ldots, t_N$ and a corresponding discrete path of the SPH system in the configuration space, given by:

$$\begin{aligned}
\mathbf{q}\left(t_0\right) &= \left(\left[\mathbf{q}^1\left(t_0\right)\right]^T, \left[\mathbf{q}^2\left(t_0\right)\right]^T, \ldots, \left[\mathbf{q}^M\left(t_0\right)\right]^T\right)^T \equiv \mathbf{q}_0, \\
\mathbf{q}\left(t_1\right) &= \left(\left[\mathbf{q}^1\left(t_1\right)\right]^T, \left[\mathbf{q}^2\left(t_1\right)\right]^T, \ldots, \left[\mathbf{q}^M\left(t_1\right)\right]^T\right)^T \equiv \mathbf{q}_1, \\
&\vdots \qquad\qquad\qquad\qquad \vdots \qquad\qquad\qquad\qquad \vdots \\
\mathbf{q}\left(t_N\right) &= \left(\left[\mathbf{q}^1\left(t_N\right)\right]^T, \left[\mathbf{q}^2\left(t_N\right)\right]^T, \ldots, \left[\mathbf{q}^M\left(t_N\right)\right]^T\right)^T \equiv \mathbf{q}_N.
\end{aligned}$$

Moreover, a numerical integration rule is necessary to approximate the action in the interval $[t_k, t_{k+1}]$. In this work we choose the generalized midpoint rule which gives [22]:

$$\begin{aligned}
L(\mathbf{q}_k^i, \mathbf{q}_{k+1}^i) &= (t_{k+1} - t_k) L\left((1-\alpha)\mathbf{q}_k^i + \alpha\mathbf{q}_{k+1}^i, \frac{\mathbf{q}_{k+1}^i - \mathbf{q}_k^i}{t_{k+1} - t_k}\right) \\
&= (t_{k+1} - t_k)\left[\frac{1}{2}\sum_i m_i\left(\frac{\mathbf{q}_{k+1}^i - \mathbf{q}_k^i}{t_{k+1} - t_k}\right)^2 - \sum_i m_i\pi(\rho_i) + \sum_i m_i((1-\alpha)\mathbf{q}_k^i + \alpha\mathbf{q}_{k+1}^i)\cdot\mathbf{g}\right],
\end{aligned} \tag{19}$$

where the Lagrangian L is defined by expression (18), the parameter $\alpha \in [0,1]$, and:

$$\rho^i_{k,k+1} = \rho((1-\alpha)\mathbf{q}^i_k + \alpha\mathbf{q}^i_{k+1}) = \sum_j m_j W_j \left((1-\alpha)\mathbf{q}^i_k + \alpha\mathbf{q}^i_{k+1} - \left((1-\alpha)\mathbf{q}^j_k + \alpha\mathbf{q}^j_{k+1}\right)\right). \quad (20)$$

So,

$$\frac{\partial L_d}{\partial \mathbf{q}^i_k}(\mathbf{q}_k, \mathbf{q}_{k+1}) = (t_{k+1} - t_k)\left[m_i\left(\frac{\mathbf{q}^i_{k+1} - \mathbf{q}^i_k}{t_{k+1} - t_k}\right)\frac{-1}{t_{k+1} - t_k} - \frac{\partial}{\partial \mathbf{q}^i_k}\sum_i m_i \pi(\rho_i) + m_i(1-\alpha)\mathbf{g}\right], \quad (21)$$

But, by using the Chain rule, the constitutive equation (17) involving pressure and density, and equation (7), we can prove that:

$$\frac{\partial}{\partial \mathbf{q}^i_k}\sum_i m_i \pi(\rho^i_{k,k+1}) = \sum_j m_i m_j \left(\frac{p^i_{k,k+1}}{\left(\rho^i_{k,k+1}\right)^2} + \frac{p^j_{k,k+1}}{\left(\rho^j_{k,k+1}\right)^2}\right)\nabla_j W(\cdot)(1-\alpha), \quad (22)$$

where:

$$\begin{aligned}
\nabla_j W(\cdot) &= \nabla_j W\left((1-\alpha)\mathbf{q}^i_k + \alpha\mathbf{q}^i_{k+1} - \left((1-\alpha)\mathbf{q}^j_k + \alpha\mathbf{q}^j_{k+1}\right)\right), & (23)\\
p^i_{k,k+1} &= p((1-\alpha)\mathbf{q}^i_k + \alpha\mathbf{q}^i_{k+1}), & (24)\\
p^j_{k,k+1} &= p\left((1-\alpha)\mathbf{q}^j_k + \alpha\mathbf{q}^j_{k+1}\right), & (25)
\end{aligned}$$

Therefore by inserting expression (22) into equation (21) we obtain:

$$\begin{aligned}
\frac{\partial L_d}{\partial \mathbf{q}^i_k}(\mathbf{q}_k, \mathbf{q}_{k+1}) &= -m_i\left(\frac{\mathbf{q}^i_{k+1} - \mathbf{q}^i_k}{\Delta t}\right) - \Delta t\sum_j m_i m_j \left(\frac{p^i_{k,k+1}}{\left(\rho^i_{k,k+1}\right)^2} + \frac{p^j_{k,k+1}}{\left(\rho^j_{k,k+1}\right)^2}\right)\nabla_j W(\cdot)(1-\alpha) & (26)\\
&\quad + \Delta t m_i(1-\alpha)\mathbf{g}, & (27)
\end{aligned}$$

where $\Delta t = (t_{k+1} - t_k) = constant$, $\nabla_j W(\cdot)$, $p^i_{k,k+1}$ and $p^j_{k,k+1}$, are defined in expressions (23), (24) and (25), respectively.

Analogously, we can calculate the action in the interval $[t_{k-1}, t_k]$ to obtain:

$$\begin{aligned}
L_d(\mathbf{q}_{k-1}, \mathbf{q}_k) &= \Delta t L\left((1-\alpha)\mathbf{q}_{k-1} + \alpha\mathbf{q}_k, \frac{\mathbf{q}_k - \mathbf{q}_{k-1}}{\Delta t}\right)\\
&= \Delta t\left[\frac{1}{2}\sum_i m_i\left(\frac{\mathbf{q}^i_k - \mathbf{q}^i_{k-1}}{\Delta t}\right)^2 - \sum_i m_i \pi(\rho^i_{k-1,k}) + \sum_i m_i((1-\alpha)\mathbf{q}^i_{k-1} + \alpha\mathbf{q}^i_k)\cdot\mathbf{g}\right], \quad (28)
\end{aligned}$$

where:

$$\rho^i_{k-1,k} = \rho\left((1-\alpha)\mathbf{q}^i_{k-1} + \alpha\mathbf{q}^i_k\right) = \sum_j m_j W\left((1-\alpha)\mathbf{q}^i_{k-1} + \alpha\mathbf{q}^i_k - \left((1-\alpha)\mathbf{q}^j_{k-1} + \alpha\mathbf{q}^j_k\right)\right). \quad (29)$$

Then, following a development analogous to the one performed to obtain expression (27) we can demonstrate that:

$$\begin{aligned}
\frac{\partial L_d}{\partial \mathbf{q}^i_k}(\mathbf{q}_{k-1}, \mathbf{q}_k) &= -m_i\left(\frac{\mathbf{q}^i_k - \mathbf{q}^i_{k-1}}{\Delta t}\right) - \Delta t\sum_j m_i m_j \left(\frac{p_i^{k-1,k}}{\left(\rho_i^{k-1,k}\right)^2} + \frac{p_j^{k-1,k}}{\left(\rho_j^{k-1,k}\right)^2}\right)\nabla_j W(\cdot\cdot)\alpha & (30)\\
&\quad + \Delta t m_i \alpha\mathbf{g}, & (31)
\end{aligned}$$

where

$$\nabla_j W(\cdot\cdot) = \nabla_j W\left((1-\alpha)\mathbf{q}^i_{k-1} + \alpha\mathbf{q}^i_k - \left((1-\alpha)\mathbf{q}^j_{k-1} + \alpha\mathbf{q}^j_k\right)\right), \tag{32}$$

and:

$$p^i_{k-1,k} = p((1-\alpha)\mathbf{q}^i_{k-1} + \alpha\mathbf{q}^i_k), \tag{33}$$

$$p^j_{k-1,k} = p\left(\left((1-\alpha)\mathbf{q}^j_{k-1} + \alpha\mathbf{q}^j_k\right)\right). \tag{34}$$

Now, if we insert expressions (27) and (31) into equation (5) and re-arrange the terms we get:

$$\frac{\mathbf{q}^i_{k+1} - 2\mathbf{q}^i_k + \mathbf{q}^i_{k-1}}{\Delta t} = \Delta t(1-\alpha)\left[-\sum_j m_j\left(\frac{p^i_{k,k+1}}{\left(\rho^i_{k,k+1}\right)^2} + \frac{p^j_{k,k+1}}{\left(\rho^j_{k,k+1}\right)^2}\right)\nabla_j W(\cdot) + \mathbf{g}\right] \tag{35}$$

$$+\Delta t\alpha\left[-\sum_j m_j\left(\frac{p^i_{k-1,k}}{\left(\rho^i_{k-1,k}\right)^2} + \frac{p^j_{k-1,k}}{\left(\rho^j_{k-1,k}\right)^2}\right)\nabla_j W(\cdot\cdot) + \mathbf{g}\right], \tag{36}$$

which defines the variational time integration scheme for SPH using the generalized midpoint rule. This numerical scheme is an implicit one, except for $\alpha \in \{0, 1\}$ which is discussed next (section 5.3).

5.1 Momentum Conservation

In the absence of external forces the total linear momentum of a mechanical system is preserved. We can use the framework of the discrete Noether's Theorem to show that the integration scheme defined by equation (36) meets these requirements [18]. On the other hand, we can follow a more direct approach. We can use expression (36) to make explicit the relationship between the momentum variation of a particle with mass m_i and the internal forces, which is given by:

$$m_i\left(\frac{\mathbf{q}^i_{k+1} - 2\mathbf{q}^i_k + \mathbf{q}^i_{k-1}}{(\Delta t)^2}\right) = (1-\alpha)\left[-\sum_j m_i m_j\left(\frac{p^i_{k,k+1}}{\left(\rho^i_{k,k+1}\right)^2} + \frac{p^j_{k,k+1}}{\left(\rho^j_{k,k+1}\right)^2}\right)\nabla_j W(\cdot)\right]$$

$$+\alpha\left[-\sum_j m_i m_j\left(\frac{p^i_{k-1,k}}{\left(\rho^i_{k-1,k}\right)^2} + \frac{p^j_{k-1,k}}{\left(\rho^j_{k-1,k}\right)^2}\right)\nabla_j W(\cdot\cdot)\right], \tag{37}$$

with $\nabla_j W(\cdot)$ and $\nabla_j W(\cdot\cdot)$ given by equations (23) and (32), respectivelly.

Due to the kernel properties [21] we can show that:

$$\nabla_j W(\cdot) = -\nabla_i W(\cdot), \quad \nabla_j W(\cdot\cdot) = -\nabla_i W(\cdot\cdot).$$

By inserting these expressions in equation (37) it is straightforward to show that:

$$\sum_i m_i\left(\frac{\mathbf{q}^i_{k+1} - 2\mathbf{q}^i_k + \mathbf{q}^i_{k-1}}{(\Delta t)^2}\right) \equiv \sum_i m_i\mathbf{a}^i = \mathbf{0},$$

which proves the preservation of linear momentum under the action of internal forces.

In order to preserve the angular momentum we need more considerations. Specifically, the discrete Noether's Theorem states that if the discrete Lagrangian L_d is invariant under the action of a transformation group, then we have conservation of the associated momentum. In our case, L_d is given by expression (19) and we shall discard the external (gravitational) field for this analysis. It is easy to show that the part of L_d that accounts for the kinetic energy is invariant under

rotations, which is the transformation group related to angular momentum. However, we need to apply specific corrections in the traditional SPH kernels and/or gradient in order to fulfill this invariance for the internal energy, as demonstrated in [4]. We are not considering such corrections in this paper and, consequently, we can not assure angular momentum conservation.

5.2 Solving implicit Scheme

In this section we re-write equation (36) as $\mathbf{q}_{k+1}^i = F\left(\mathbf{q}_{k+1}^i, \mathbf{q}_k^i, \mathbf{q}_{k-1}^i\right)$ and we suppose that $\mathbf{q}_k^i$, $\mathbf{q}_{k-1}^i$ are known. Therefore, we have $F : \mathbb{R}^3 \to \mathbb{R}^3$ and we can seek for conditions for which F becomes a contraction mapping respect to the unknown $\mathbf{q}_{k+1}^i$. In this way, we can find the solution of equation (36) through a fixed point iterative algorithm that is simpler to implement than the traditional Newton's method [22]. To prove that F is contraction, we should find a constant $c \in [0, 1)$ satisfying:

$$d\left(F\left((\mathbf{q}_{k+1}^i)_1, \mathbf{q}_k^i, \mathbf{q}_{k-1}^i\right), F\left((\mathbf{q}_{k+1}^i)_2, \mathbf{q}_k^i, \mathbf{q}_{k-1}^i\right)\right) \leq cd\left((\mathbf{q}_{k+1}^i)_1, (\mathbf{q}_{k+1}^i)_2\right),$$

where $d : \mathbb{R}^3 \times \mathbb{R}^3 \to \mathbb{R}^+$ is a convenient distance function and $(\mathbf{q}_{k+1}^i)_1, (\mathbf{q}_{k+1}^i)_2 \in \mathbb{R}^3$.

So, from equation (36) it is straightforward to show that:

$$F\left(\mathbf{q}_{k+1}^i, \mathbf{q}_k^i, \mathbf{q}_{k-1}^i\right) = 2\mathbf{q}_k^i - \mathbf{q}_{k-1}^i + (\Delta t)^2 (1-\alpha) H_g\left(\mathbf{q}_{k+1}^i, \mathbf{q}_k^i\right) + (\Delta t)^2 \alpha H_g\left(\mathbf{q}_k^i, \mathbf{q}_{k-1}^i\right), \quad (38)$$

where:

$$H_g\left(\mathbf{q}_{k+1}^i, \mathbf{q}_k^i\right) = \left[-\sum_j m_j \left(\frac{p_{k,k+1}^i}{\left(\rho_{k,k+1}^i\right)^2} + \frac{p_{k,k+1}^j}{\left(\rho_{k,k+1}^j\right)^2}\right) \nabla_j W(\cdot) + \mathbf{g}\right], \quad (39)$$

$$H_g\left(\mathbf{q}_k^i, \mathbf{q}_{k-1}^i\right) = \left[-\sum_j m_j \left(\frac{p_i^{k-1,k}}{\left(\rho_i^{k-1,k}\right)^2} + \frac{p_j^{k-1,k}}{\left(\rho_j^{k-1,k}\right)^2}\right) \nabla_j W(\cdot\cdot) + \mathbf{g}\right], \quad (40)$$

and $\nabla_j W(\cdot)$ and $\nabla_j W(\cdot\cdot)$ are defined by equations (23) and (32), respectively.

From the traditional calculus we know that if $f : U \subset \mathbb{R}^n \to \mathbb{R}^n$ is differentiable with $\|\partial f/\partial x\| \leq M_1$ for any $x \in U$ then f is Lipschitz; that means, $\|f(y) - f(x)\| \leq M_1 \|y - x\|$, $\forall x, y \in U$. If we show that F is Lipschitz then our problem turns out in finding conditions to assure that $0 \leq M_1 < 1$ in order to apply a fixed point iterative method to approximate the solution of the equation (36). Moreover, the derivative of F respect to $\mathbf{q}_{k+1}^i$ is:

$$\frac{\partial F}{\partial \mathbf{q}_{k+1}^i} = (\Delta t)^2 (1-\alpha) \frac{\partial H_g}{\partial \mathbf{q}_{k+1}^i}(\mathbf{q}_{k+1}, \mathbf{q}_k) \quad (41)$$

where $H_g\left(\mathbf{q}_{k+1}^i, \mathbf{q}_k^i\right)$ is define by equation (39). To demonstrate that expression (41) is limited, we need to prove that the density and pressure are limited fields. The density $\rho_{k,k+1}^i = \rho((1-\alpha)\mathbf{q}_k^i + \alpha \mathbf{q}_{k+1}^i)$ is computed by expression (20). Once the kernel W is limited ($W(R) \leq \ell$ in expression (10)), we can write:

$$\rho_{k,k+1}^i = \sum_{j=1}^M m_j W(\cdot) \leq \sum_{j=1}^M m_j \ell = c_\rho, \quad (42)$$

where c_ρ is a constant. On the other hand, the pressure $p_{k,k+1}^i = p((1-\alpha)\mathbf{q}_k^i + \alpha \mathbf{q}_{k+1}^i)$ is given by the state equation (11):

$$p_{k,k+1}^i = B\left[\left(\frac{\sum_{j=1}^M m_j W(\cdot)}{\rho_0}\right)^7 - 1\right] \leq B\left[\left(\frac{c_\rho}{\rho_0}\right)^7 - 1\right] = c_p \quad (43)$$

with c_p being constant. Consequently:

$$\begin{aligned}\left|\frac{p^i_{k,k+1}}{(\rho^i_{k,k+1})^2}\right| &= \left|B\left[\frac{(\rho^i_{k,k+1})^5}{(\rho_0)^7}-\frac{1}{(\rho^i_{k,k+1})^2}\right]\right| \\ &\leq \left|\frac{B(\rho^i_{k,k+1})^5}{(\rho_0)^7}\right|+\left|\frac{B}{(\rho^i_{k,k+1})^2}\right| \leq \left|\frac{B(c_\rho)^5}{(\rho_0)^7}\right|+\left|\frac{B}{(m_i\ell)^2}\right| = k_i. \end{aligned} \tag{44}$$

Therefore, we can now seek for a bound for expression:

$$\frac{\partial H_g}{\partial \mathbf{q}^i_{k+1}}(\mathbf{q}_{k+1},\mathbf{q}_k) = -\sum_{j=1}^{M} m_j \frac{\partial}{\partial \mathbf{q}^i_{k+1}}\left(\frac{p^i_{k,k+1}}{\left(\rho^i_{k,k+1}\right)^2}+\frac{p^j_{k,k+1}}{\left(\rho^j_{k,k+1}\right)^2}\right)\nabla_j W(\cdot) \tag{45}$$

$$-\sum_{j=1}^{M} m_j \left(\frac{p^i_{k,k+1}}{\left(\rho^i_{k,k+1}\right)^2}+\frac{p^j_{k,k+1}}{\left(\rho^j_{k,k+1}\right)^2}\right)\frac{\partial}{\partial \mathbf{q}^i_{k+1}}\nabla_j W(\cdot), \tag{46}$$

where:

$$\nabla_j W(\cdot) = \frac{\partial}{\partial \mathbf{q}^j_k} W(\cdot) = (1-\alpha)2ce^{-R^2}\left[(1-\alpha)\mathbf{q}^i_k+\alpha\mathbf{q}^i_{k+1}-\left((1-\alpha)\mathbf{q}^j_k+\alpha\mathbf{q}^j_{k+1}\right)\right].$$

The analysis of the first term in equation (46) can be made by considering the general term:

$$\begin{aligned}\frac{\partial}{\partial \mathbf{q}^s_{k+1}}\left(\frac{p_i^{k,k+1}}{\left(\rho_i^{k,k+1}\right)^2}\right) &= \frac{\partial}{\partial \mathbf{q}^s_{k+1}}\left(B\left[\frac{1}{(\rho_0)^2}\left(\frac{\rho^i_{k,k+1}}{\rho_0}\right)^5-\frac{1}{\left(\rho_i^{k,k+1}\right)^2}\right]\right) \\ &= \frac{5B}{(\rho_0)^2}\left(\frac{\sum_{j=1}^M m_j W(\cdot)}{\rho_0}\right)^4 \times \frac{\left(\sum_{j=1}^M m_j \frac{\partial}{\partial \mathbf{q}^s_{k+1}} W(\cdot)\right)}{\rho_0} \\ &\quad +2B\frac{\sum_{j=1}^M m_j \frac{\partial}{\partial \mathbf{q}^s_{k+1}} W(\cdot)}{\left(\rho_i^{k,k+1}\right)^3}. \end{aligned} \tag{47}$$

Expression (47) depends on basic operations involving the density ρ, which is limited by c_ρ, the Gaussian kernel W (expression (10)), and its first order derivatives which are also limited. The second term of equation (46) includes derivatives of second order of the Gaussian kernel W:

$$\begin{aligned}\frac{\partial}{\partial \mathbf{q}^i_{k+1}}\nabla_j W(\cdot) &= \frac{\partial}{\partial \mathbf{q}^i_{k+1}}\frac{\partial}{\partial \mathbf{q}^j_k} W((1-\alpha)\mathbf{q}^i_k+\alpha\mathbf{q}^i_{k+1}-\left((1-\alpha)\mathbf{q}^j_k+\alpha\mathbf{q}^j_{k+1}\right)) \\ &= -2\alpha\frac{\partial W(R)}{\partial \mathbf{q}^i_{k+1}}\left[(1-\alpha)\mathbf{q}^i_k+\alpha\mathbf{q}^i_{k+1}-\left((1-\alpha)\mathbf{q}^j_k+\alpha\mathbf{q}^j_{k+1}\right)\right] \\ &\quad -2c\alpha e^{-R^2}\frac{\partial}{\partial \mathbf{q}^i_{k+1}}\left[(1-\alpha)\mathbf{q}^i_k+\alpha\mathbf{q}^i_{k+1}-\left((1-\alpha)\mathbf{q}^j_k+\alpha\mathbf{q}^j_{k+1}\right)\right], \end{aligned} \tag{48}$$

that are also limited. This fact together with expression (44) demonstrate that the second term in equation (46) is also limited. Therefore, considering these results we claim that there is a constant M_2 such that:

$$\left\|\frac{\partial H_g}{\partial \mathbf{q}^i_{k+1}}\left(\mathbf{q}^i_{k+1},\mathbf{q}^i_k\right)\right\| < M_2. \tag{49}$$

Consequently:

$$\left\| \frac{\partial F}{\partial \mathbf{q}^i_{k+1}} \right\| = \left\| (\Delta t)^2 (1-\alpha) \frac{\partial H_g}{\partial \mathbf{q}^i_{k+1}} (\mathbf{q}_{k+1}, \mathbf{q}_k) \right\| \leq (\Delta t)^2 (1-\alpha) M_2 \equiv M_1,$$

that means, F is Lipschitz. As a consequence of the theorem above stated we can write:

$$\left\| F\left((\mathbf{q}^i_{k+1})_1, \mathbf{q}^i_k, \mathbf{q}^i_{k-1}\right) - F\left((\mathbf{q}^i_{k+1})_2, \mathbf{q}^i_k, \mathbf{q}^i_{k-1}\right) \right\| \leq M_1 \|(\mathbf{q}^i_{k+1})_1 - (\mathbf{q}^i_{k+1})_2\|.$$

To assure that the function F in expression (38) is a contraction mapping we need to satisfy $M_1 \leq 1$, which implies:

$$\Delta t < \frac{1}{\sqrt{(1-\alpha) M_2}}. \tag{50}$$

This equation gives the range for Δt that allow to apply the fixed point framework to solve the implicit integrator given by expression (36). The practical consequences of the bound given above is application dependent and its utility will be analysed in the experimental results.

5.3 Implementation Details

Before simulating SPH with expression (36), we need to add extra machinery to account for numerical aspects and interaction of particles with boundary. In order to consider the former, let us set $\alpha = 0$ in expression (36). From equation (24) we shall notice that $p^i_{k,k+1} = p(\mathbf{q}^i_k)$, if $\alpha = 0$. Besides, if we set $\alpha = 1$ in equation (33) we get also $p^i_{k-1,k} = p(\mathbf{q}^i_k)$. Analogous results are obtained for $\rho^i_{k,k+1}$ and $\rho^i_{k-1,k}$ in expressions (20), (29), respectively. As a consequence, we obtain the same explicit integration scheme for both $\alpha = 1$ and $\alpha = 0$ in expression (36), given by:

$$\frac{\mathbf{q}^i_{k+1} - 2\mathbf{q}^i_k + \mathbf{q}^i_{k-1}}{\Delta t} = \Delta t \left[-\sum_j m_j \left(\frac{p(\mathbf{q}^i_k)}{\left(\rho(\mathbf{q}^i_k)\right)^2} + \frac{p(\mathbf{q}^j_k)}{\left(\rho(\mathbf{q}^j_k)\right)^2} \right) \nabla_j W(\mathbf{q}^i_k - \mathbf{q}^j_k) + \mathbf{g} \right]. \tag{51}$$

In order to add stability to the scheme defined by expression (51) we follow [20] and include the artificial viscosity:

$$\Pi^{ij}_{k-1,k} = \begin{cases} \dfrac{-2(a\varphi_{ij} c + b\varphi^2_{ij})}{\rho^i_{k-1,k} + \rho^j_{k-1,k}}, & \mathbf{v}^{ij}_{k-1,k} \cdot \mathbf{x}^{ij}_k < 0 \\ 0, & \mathbf{v}^{ij}_{k-1,k} \cdot \mathbf{x}^{ij}_k \geq 0 \end{cases} \quad \text{and } \alpha_{ij} = \frac{(\mathbf{v}^{ij}_{k-1,k} \cdot \mathbf{x}^{ij}_k) h}{\left(r^{ij}_k\right)^2 + 0.01 h^2} \tag{52}$$

where:

$$\mathbf{v}^{ij}_{k-1,k} = \mathbf{v}^i_{k-1,k} - \mathbf{v}^j_{k-1,k}, \tag{53}$$

with:

$$\mathbf{v}^i_{k-1,k} = \frac{\mathbf{q}^i_k - \mathbf{q}^i_{k-1}}{\Delta t}, \tag{54}$$

and $\mathbf{x}^{ij}_k = \mathbf{q}^i_k - \mathbf{q}^j_k$, $r^{ij}_k = \|\mathbf{x}^{ij}_k\|$ ($\|\cdot\|$ means the Euclidean norm). The a and b are constants that are all typically set around 1, the constants c and h represent the speed of sound and smoothing length, respectively,

Besides, we shall consider repulsive boundary forces to prevent the interior particle from penetrating the boundary of the domain. In this work this is implemented using boundary particles

that do not move but interact with fluid particles [20]. Specifically, if a boundary particle $\mathbf{q}^g$ is in the neighborhood of a real particle $\mathbf{q}_k^i$ that is approaching the boundary, then the force:

$$\Gamma_k^{ig} = \begin{cases} D\left[\left(\dfrac{r_0}{r_k^{ig}}\right)^{n_1} - \left(\dfrac{r_0}{r_k^{ig}}\right)^{n_2}\right] & \dfrac{r_0}{r_k^{ig}} \leq 1 \\ 0 & \dfrac{r_0}{r_k^{ig}} > 1 \end{cases} \tag{55}$$

is applied pairwisely along the centerline of these two particles, where $n_1 = 12$, $n_2 = 4$, $r_k^{ig} = \|\mathbf{q}_k^i - \mathbf{q}^g\|$, and r_0 is usually selected close to the initial particles spacing. The parameter D is problem dependent, and its value should be chosen with the same order of the square of the largest velocity.

If we add expressions (52) and (55) to the right hand side of equation (51) then we can define:

$$\mathbf{a}^i = -\sum_j m_j \left(\frac{p(\mathbf{q}_k^i)}{\left(\rho(\mathbf{q}_k^i)\right)^2} + \frac{p(\mathbf{q}_k^j)}{\left(\rho(\mathbf{q}_k^j)\right)^2}\right) \nabla_j W(\mathbf{q}_k^i - \mathbf{q}_k^j) + \sum_j \Pi_{k-1,k}^{ij} \nabla_j W(\mathbf{q}_k^i - \mathbf{q}_k^j) + \Gamma_k^{ig} + \mathbf{g}, \tag{56}$$

and compute the solution $\mathbf{q}_{k+1}^i$ using the iterative procedure:

$$\mathbf{v}^i\left(k - \frac{1}{2}\Delta t\right) = \frac{\mathbf{q}_k^i - \mathbf{q}_{k-1}^i}{\Delta t}, \tag{57}$$

$$\mathbf{v}^i\left(k + \frac{1}{2}\Delta t\right) = \mathbf{v}^i(k - \frac{1}{2}\Delta t) + \Delta t \mathbf{a}^i, \tag{58}$$

$$\mathbf{q}_{k+1}^i = \mathbf{q}_k^i + \Delta t \mathbf{v}^i\left(k + \frac{1}{2}\Delta t\right) \tag{59}$$

for $k = 1, 2, \ldots, N$. If $k = 0$ in equation (57) then we set $\mathbf{v}^i(-1/2) = v_i(0) - (1/2)\Delta t \mathbf{g}$. Expressions (57)-(59) defines the traditional Verlet (or Leapfrog) algorithm in the SPH literature [28, 20].

Moreover, to include the effects of viscous and boundary interaction in the implicit SPH model defined by expression (36) with $0 < \alpha < 1$, without creating asymmetric effects, we propose in this work the following scheme:

$$\frac{\mathbf{q}_{k+1}^i - 2\mathbf{q}_k^i + \mathbf{q}_{k-1}^i}{\Delta t} = \Delta t(1-\alpha)\mathbf{a}_1^i + \Delta t \alpha \mathbf{a}_2^i \tag{60}$$

where:

$$\mathbf{a}_1^i = -\sum_j m_j \left(\frac{p_{k,k+1}^i}{\left(\rho_{k,k+1}^i\right)^2} + \frac{p_{k,k+1}^j}{\left(\rho_{k,k+1}^j\right)^2}\right) \nabla_j W(\cdot) + \sum_j m_j \Pi_k^{ij} \nabla_j W(\cdot) + \Gamma_k^{ig} + \mathbf{g}, \tag{61}$$

$$\mathbf{a}_2^i = -\sum_j m_j \left(\frac{p_{k-1,k}^i}{\left(\rho_{k-1,k}^i\right)^2} + \frac{p_{k-1,k}^j}{\left(\rho_{k-1,k}^j\right)^2}\right) \nabla_j W(\cdot\cdot) + \sum_j m_j \Pi_k^{ij} \nabla_j W(\cdot\cdot) + \Gamma_k^{ig} + \mathbf{g}. \tag{62}$$

The direct computation of the fluid density ρ using equation (8) is not recommended due to computational and precision problems. Therefore, following [29], we update the density field using the continuity equation:

$$\frac{D\rho}{Dt} = -\rho \nabla \cdot \mathbf{v}. \tag{63}$$

Using equation (9) to write the kernel version of the right hand side of expression (63) and finite differences to approximate the left hand side of this expression we get:

$$\frac{\rho^i_{k,k+1} - \rho^i_{k-1,k}}{\Delta t} = -\sum_j m_j \mathbf{v}^{ij}_{k,k+1} \cdot \nabla_i W\left((1-\alpha)\mathbf{q}^i_k + \alpha \mathbf{q}^i_{k+1} - \left((1-\alpha)\mathbf{q}^j_k + \alpha \mathbf{q}^j_{k+1}\right)\right), \quad (64)$$

$$\frac{\rho^i_{k-1,k} - \rho^i_{k-2,k-1}}{\Delta t} = -\sum_j m_j \mathbf{v}^{ij}_{k-1,k} \cdot \nabla_i W\left((1-\alpha)\mathbf{q}^i_{k-1} + \alpha \mathbf{q}^i_k - \left((1-\alpha)\mathbf{q}^j_{k-1} + \alpha \mathbf{q}^j_k\right)\right), \quad (65)$$

where $\mathbf{v}^{ij}_{k-1,k}$ and $\mathbf{v}^{ij}_{k,k+1}$ are given by expression (53).

The expressions that appear in the SPH computation evaluate the kernel W, or its derivatives, in the particles positions. In order to avoid unnecessary computational overload, we set a smoothing length h that prunes the support of the kernel as follows:

$$W(R) = \begin{cases} \ell e^{-R^2}, \ if & R \leq h \\ \\ 0, & otherwise. \end{cases} \quad (66)$$

The SPH procedure is summarized by the Algorithm 1.

Algorithm 1 Algorithm for implicit SPH computation.

(a) Parameters: Particle mass m, number of particles M, number of iterations N, time step Δt, α, tolerance ε;
(b) Initial conditions $\mathbf{q}^i_0$, $\mathbf{q}^i_1$, $i = 1, \cdots, M$;
for $k = 1, 2, \ldots, N-1$ **do**
    Guess $\mathbf{q}^i_{k+1,0}$; $i = 1, \cdots, M$.
    for $i = 1, 2, \ldots, M$ **do**
        for $j = 1, 2 \ldots$ **do**
            $\mathbf{q}^i_{k+1;j} = F\left(\mathbf{q}^i_{k+1;j-1}, \mathbf{q}^i_k, \mathbf{q}^i_{k-1}, \alpha\right)$,
            if $\|\mathbf{q}^i_{k+1;j} - \mathbf{q}^i_{k+1;j-1}\| \leq \varepsilon$ **then**
                $\mathbf{q}^i_{k+1} \leftarrow \mathbf{q}^i_{k+1;j}$
                break
            end if
        end for
    end for
end for

procedure COMPUTE F$(\mathbf{q}^i_{k+1;j-1}, \mathbf{q}^i_k, \mathbf{q}^i_{k-1}, \alpha)$
    Calculate densities $\rho^i_{k,k+1;j-1}$ and $\rho^i_{k-1,k;j-1}$ through expressions (64) and (65);
    Compute pressures $p^i_{k,k+1;j-1}$ and $p^i_{k-1,k;j-1}$ using expressions (24), (33) and the state equation (11);
    Calculate artificial viscosity $\Pi^{ij}_{k,k+1}$ and boundary forces Γ^{ig}_k using expressions (52) and (55);
    Compute $\mathbf{a}^i_1$ and $\mathbf{a}^i_2$ through expressions (61)-(62)
    Evaluate and return:

$$F\left(\mathbf{q}^i_{k+1;j-1}, \mathbf{q}^i_k, \mathbf{q}^i_{k-1}\right) = (\Delta t)^2\left((1-\alpha)\mathbf{a}^i_1 + \alpha \mathbf{a}^i_2\right) + 2\mathbf{q}^i_k - \mathbf{q}^i_{k-1}.$$

end procedure

In this algorithm we follow the idea of section 5.2 and compute the position of the particle i at time $t = k+1$ through an iteration scheme based on the fixed point method. The index j is related to the fixed point iteration. Hence, we start with an initial guess for $\mathbf{q}^i_{k+1}$, named $\mathbf{q}^i_{k+1,0}$

in line 4 of Algorithm 1, which is updated in each iteration j of the successive approximations computed in lines 5-13 of Algorithm 1, until the stopping criterion in line 8 is achieved. The function F in line 7 is implemented following the procedure $Compute\, F(\mathbf{q}^i_{k+1;j-1}, \mathbf{q}^i_k, \mathbf{q}^i_{k-1}, \alpha)$ just bellow the Algorithm 1.

6 Computational Experiments

In this section we test the time integration scheme computed by Algorithm 1. In these experiments we highlight aspects of the fixed point iteration procedure, comparison with the Verlet (expressions (57)-(59)) and momentum conservation.

We use the dam breaking simulation as the numerical example to test the evolution of the SPH system computed by the time integration scheme in expression (60) for $\alpha = 0.5$. Although idealized, the dam breaking configuration contains information that allow engineers to know what will happen if a dam fails and how to set up numerical models to test it. For SPH purposes the dam breaking set up is interesting to test the numerical stability and balance of internal forces in the fluid.

In the computational experiments performed we use $M = 1682$ SPH particles, each one with mass $0.025kg$. The smoothing length and the parameter ℓ in expression (66) are set to $h = 0.072$ and $\ell = 9,47$. The rest density and gravitational field intensity are given by $\rho 0 = 1000.0kg/m^3$ and $g = 9.8m/s^2$, respectively. The values for the tolerance used in line 8 of the Algorithm 1 is $\varepsilon = 0.001$.

The computational domain, shown in Figure 1, is a rectangular region with dimensions $R_x = 0.58m$ and $R_y = 0.29m$. The initial dam, shown in Figure 1, is a fluid column with width $0.145m$ and high $0.29m$ filled by a regular distribution of SPH particles with 58×29 particles.

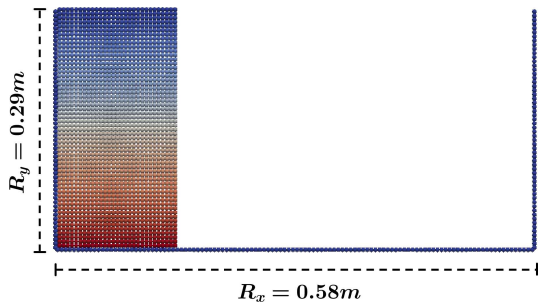

Figure 1: Configuration for dam breaking simulation.

Firstly, we should compute the bound for the time step Δt through equation (50). Due to expression (66), the bound c_ρ in (42) depends on the estimation of the number of particles in the neighborhood $\mathcal{B}^i(h) = \{\mathbf{q}^j; \|\mathbf{q}^i - \mathbf{q}^j\| \leq h\}$ of a generic particle $\mathbf{q}^i$. Considering the dimensions of the initial dam and the number of particles, we postulate that the cardinality of $\mathcal{B}^i(h)$ has the upper bound given by $card\,(\mathcal{B}^i(h)) \approx \mathcal{O}(10^1)$. Therefore $\rho^i_{k,k+1} \leq c_\rho \approx \mathcal{O}(10^4)$, due to expression (42). By substituting this result in equation (43) and using the fact that $B = c^2\rho_0/7$ in this expression, we obtain $c_p \approx \mathcal{O}(10^{12})$.

By substituting the bounds for c_ρ, c_p in equations (46)-(48), and by computing the bounds for the first and second kernel derivatives, we get after some algebra that $M_2 \approx \mathcal{O}(10^9)$ and, consequently, $\Delta t \leq 10^{-4}$ is enough to apply the fixed point procedure. Therefore, if we set $\Delta t = 0.0001s$ in initialization of the Algorithm 1, we satisfy the condition (50).

The Figures 2.(a)-(d) show some snapshots of the fluid motion with the collapse of the rectangular $2D$ dam due to the action of the gravity field. The simulation is performed using the implicit scheme described by the Algorithm 1, with $\alpha = 0.5$.

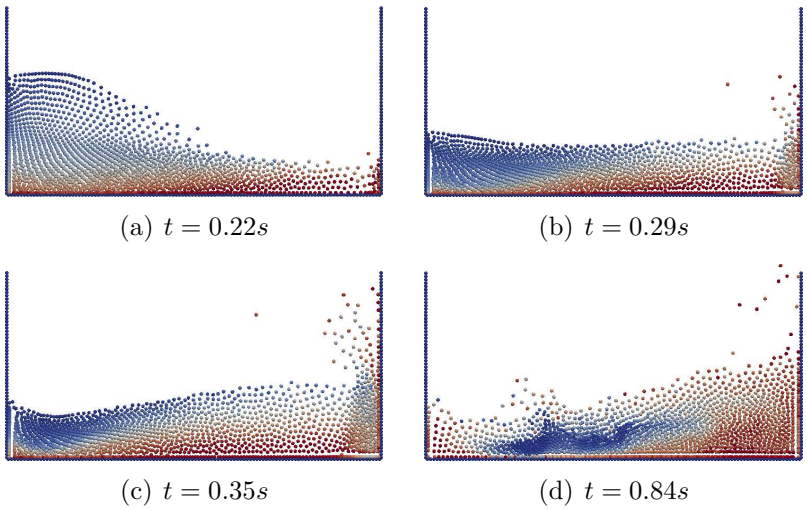

(a) $t = 0.22s$ (b) $t = 0.29s$

(c) $t = 0.35s$ (d) $t = 0.84s$

Figure 2: Dam breaking flow configuration for $\alpha = 0.5$ at time steps.

We also simulate the explicit scheme obtained by setting $\alpha \in \{0, 1\}$ in expression (60) in order to compare a traditional SPH solution with the implicit one. With this comparison we can visualize the differences between the implicit and explicit simulations.

The computation for $\alpha \in \{0, 1\}$ basically follows the Algorithm 1 but the fixed point iterations (lines 5-13) are replaced by a direct computation of $\mathbf{q}_{k+1}^i$ through equations (57)-(59), with $\mathbf{a}^i$ calculated by expression (56). The obtained explicit integration is computed using the same SPH and numerical parameters as before. The gravity field intensity and the kernel are also defined like in the implicit case. The Figure 3 shows four time iterations of the simulation.

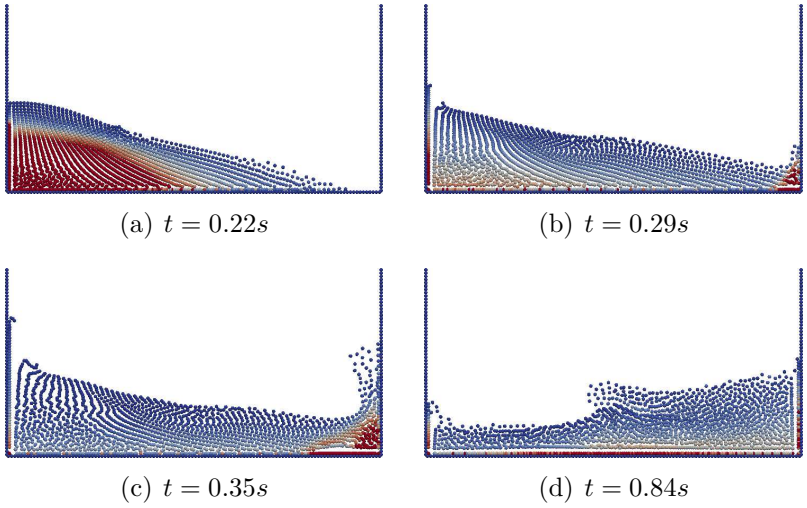

(a) $t = 0.22s$ (b) $t = 0.29s$

(c) $t = 0.35s$ (d) $t = 0.84s$

Figure 3: Dam breaking flow simulation for $\alpha \in \{0, 1\}$ at time steps.

When observing the results of Figures 2 and 3 we notice that some particles go out the fluid volume, mainly in Figures 2.(b)-(d). Particles in the SPH fluid are subject to forces from neighboring particles. Inside the fluid these inter particle forces are added and the resultant gives the fluid motion. However, the net forces acting on particles at the free surface may yield a resultant in the direction of the outward surface normal, a known problem in the SPH literature [19], which is responsibly for the phenomena observed in Figures 2. This problem can be addressed by using an additional force field, a surface tension, as a function of the curvature of the free surface or even improved versions of SPH [20, 7]. We are not considering such approaches in this paper.

The Figure (4) helps to compare the simulations for $\alpha = 0.5$ and $\alpha \in \{0, 1\}$. In this figure we

plot the quantity $D(k)$ computed as follows:

$$D(t) = max_{1 \leq i \leq M} \left\| \mathbf{q}^i_{t;imp} - \mathbf{q}^i_{t;exp} \right\|, \tag{67}$$

that means, given a time t, for each SPH particle in the implicit simulation ($\alpha = 0.5$), named $\mathbf{q}^i_{k;imp}$ above, we take the corresponding SPH particles in the explicit one ($\mathbf{q}^i_{k;exp}$), compute the distance between them and keep the maximum distance, which is plotted in Figure (4).

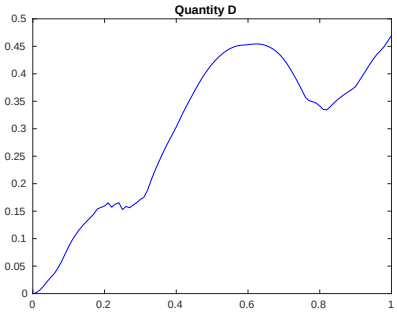

Figure 4: Time evolution of expression (67).

Although we can notice some oscillation of $D(t)$ it is clear the increasing of this quantity along the simulation, which agrees with the differences observed in the snapshots of Figures 2 and 3.

In section 5.1 we demonstrate that the linear momentum of the SPH system is preserved by equation (36). However, the SPH integrator defined by expression (60) includes boundary effects and the artificial viscosity. So, we shall analyse the consequences of these extra elements for the momentum conservation. The Figure (5) shows the temporal evolution of the linear momentum L for the dam breaking SPH simulation, given by:

$$Q = \left\| \frac{1}{M} \sum_{i=1}^{M} m_i \mathbf{v}^i_k \right\|,$$

where the velocity field is obtained by simulating the fluid using the implicit scheme (back line) and the explicit one (red line). We notice that linear momentum of the system oscillates and decays for both implicit and explicit schemes. It is an expected effect once the artificial viscosity dissipates the kinetic energy of the system. However, this effect is more intense in the explicit formulation as we can see in the interval $0.8s < t < 1.0s$.

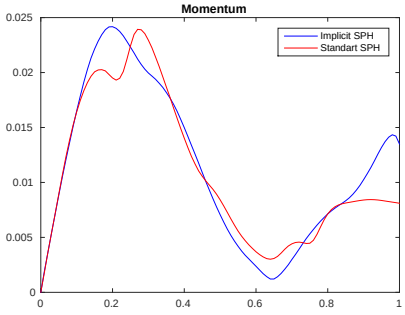

Figure 5: Linear momentum for dam breaking simulation.

7 Conclusions and Future Works

The paper has presented a discrete variational formulation for fluid simulation based on SPH. Up to the best of our knowledge, this paper is the first one to propose such discrete setting for fluid simulation within SPH framework. We demonstrate that the obtained variational time integrator preserves linear momentum. Moreover, we find conditions that support the application of fixed point theory for time integration. Due to numerical and practical requirements, we add viscous and boundary effects to the integration procedure. Therefore, we perform computational experiments to analyse the consequences of these extra machinery in the conservation property. We noticed a decreasing in the linear momentum which is less noticeable for the implicit integrator.

The midpoint numerical integration rule applied depends on a parameter α which falls in the range $[0, 1]$. Further works, that analyse topological properties of the phase space when changing the parameter α are currently under consideration.

References

[1] John D Anderson, Joris Degroote, Gérard Degrez, Erik Dick, Roger Grundmann, and Jan Vierendeels. *Computational fluid dynamics: an introduction*. Springer, 2009. 1

[2] B Ataie-Ashtiani and Leila Farhadi. A stable moving-particle semi-implicit method for free surface flows. *Fluid Dynamics Research*, 38(4):241, 2006. 1

[3] J. Bonet, S. Kulasegaram, M.X. Rodriguez-Paz, and M. Profit. Variational formulation for the smooth particle hydrodynamics (sph) simulation of fluid and solid problems. *Computer Methods in Applied Mechanics and Engineering*, 193(12–14):1245–1256, 2004. 2, 3, 5, 6

[4] J. Bonet and T.-S.L. Lok. Variational and momentum preservation aspects of smooth particle hydrodynamic formulations. *Computer Methods in Applied Mechanics and Engineering*, 180(1–2):97–115, 1999. 2, 3, 5, 6, 9

[5] Bastien Chopard, Pascal Luthi, and Alexandre Masselot. Cellular automata and lattice boltzmann techniques: An approach to model and simulate complex systems. In *Advances in Physics*, 1998. 1

[6] Leonardo Colombo, David Martín de Diego, and Marcela Zuccalli. Higher-order discrete variational problems with constraints. *Journal of Mathematical Physics*, 54(9):–, 2013. 3

[7] Jiannong Fang, Aurèle Parriaux, Martin Rentschler, and Christophe Ancey. Improved sph methods for simulating free surface flows of viscous fluids. *Appl. Numer. Math.*, 59(2):251–271, February 2009. 15

[8] E.S. Gawlik, P. Mullen, D. Pavlov, J.E. Marsden, and M. Desbrun. Geometric, variational discretization of continuum theories. *Physica D: Nonlinear Phenomena*, 240(21):1724–1760, October 2011. 3

[9] R.A. Gingold and J.J. Monaghan. Smoothed particle hydrodynamics: theory and application to non-spherical stars. *Mon. Not. Roy. Astron. Soc.*, 181:375–389, 1977. 2

[10] H. Goldstein. *Classical Mechanics*. Addison-Wesley, 2nd edition, 1981. 2, 3, 4

[11] E. Hairer, C. Lubich, and G. Wanner. *Geometric Numerical Integration: Structure-Preserving Algorithms for Ordinary Differential Equations*. Springer-Verlag, New York, 2002. 2, 3

[12] C. Kane, J. E. Marsden, M. Ortiz, and M. West. Variational integrators and the newmark algorithm for conservative and dissipative mechanical systems. *Internat. J. Numer. Methods Engrg*, 49:1295–1325, 1999. 3

[13] Liliya Kharevych, Weiwei Yang, Yiying Tong, Eva Kanso, Jerrold E. Marsden, Peter Schröder, and Mathieu Desbrun. Geometric, variational integrators for computer animation. In Carol O'Sullivan and Frederic H. Pighin, editors, *Symposium on Computer Animation*, pages 43–51. Eurographics Association, 2006. 3

[14] Kyung Sung Kim, Moo Hyun Kim, and Jong-Chun Park. Development of moving particle simulation method for multiliquid-layer sloshing. *Mathematical Problems in Engineering*, page 13, 2014. 1

[15] T. Lee, M. Leok, and N. H. McClamroch. Lie group variational integrators for the full body problem in orbital mechanics. *Celestial Mechanics and Dynamical Astronomy*, 98(2):121–144, 2007. 3

[16] T. Lee, M. Leok, and N. H. McClamroch. Lagrangian mechanics and variational integrators on two-spheres. *International Journal for Numerical Methods in Engineering*, 79(9):1147–1174, 2009. 3

[17] A. Lew, J. E. Marsden, M. Ortiz, and M. West. Variational time integrators. *International Journal for Numerical Methods in Engineering*, 60(1):153–212, 2004. 3

[18] A.J. Lew, California Institute of Technology. Division of Engineering, and Applied Science. *Variational Time Integrators in Computational Solid Mechanics*. CIT theses. California Institute of Technology, 2003. 2, 3, 8

[19] S. J. Lind, R. Xu, P. K. Stansby, and B. D. Rogers. Incompressible smoothed particle hydrodynamics for free-surface flows: A generalised diffusion-based algorithm for stability and validations for impulsive flows and propagating waves. *J. Comput. Phys.*, 231(4):1499–1523, February 2012. 15

[20] G.R. Liu and B. Liu. *Smoothed Particle Hydrodynamics: A Meshfree Particle Method*. World Scientific, 2003. 1, 5, 11, 12, 15

[21] M.B. Liu, G.R. Liu, and K.Y. Lam. Constructing smoothing functions in smoothed particle hydrodynamics with applications. *Journal of Computational and Applied Mathematics*, 155(2):263 – 284, 2003. 8

[22] J. E. Marsden and M. West. Discrete mechanics and variational integrators. *Acta Numerica*, 10:357–514, May 2001. 2, 3, 4, 6, 9

[23] Pablo Mata and Adrian J. Lew. Variational integrators for the dynamics of thermo-elastic solids with finite speed thermal waves. *J. Comput. Phys.*, 257:1423–1443, January 2014. 3

[24] J. J. Monaghan. Smoothed particle hydrodynamics and its diverse applications. *Annual Review of Fluid Mechanics*, 44(1):323–346, 2012. 2

[25] J.J. Monaghan. Smoothed particle hydrodynamics. *Ann. Rev. Astron. Astrophys.*, 30:543–74, 1992. 2

[26] Patrick Mullen, Keenan Crane, Dmitry Pavlov, Yiying Tong, and Mathieu Desbrun. Energy-preserving integrators for fluid animation. *ACM Trans. Graph.*, 28(3):38:1–38:8, July 2009. 3

[27] S. Muller and M. Ortiz. On the γ-convergence of discrete dynamics and variational integrators. *Journal of Nonlinear Science*, 14(3):279–296, 2004. 3

[28] D. Violeau. *Fluid Mechanics and the SPH Method*. Oxford University Press, 2012. 3, 12

[29] Ihmsen, Markus and Cornelis, Jens and Solenthaler, Barbara and Horvath, Christopher and Teschner, Matthias. *Implicit Incompressible SPH* IEEE Transactions on Visualization and Computer Graphics, 12